# Application Of Silica Nanoparticles And Anionic Surfactant With Low-Salinity Water To Enhance Oil Recovery In Assam Shelf Basin

## Joyshree Barman<sup>1</sup>, Prasenjit Talukdar<sup>2\*</sup>

<sup>1, 2</sup>Department of Petroleum Engineering, DUIET, Dibrugarh University, Assam-786004, India

\*Corresponding author: prasenjit duiet@dibru.ac.in

Surfactant flooding is one of the known Chemical Enhanced Oil Recovery (CEOR) techniques used in the oil and gas industry for decades. Adsorption of surfactant onto the reservoir rock surfaces limits the efficiency of the CEOR method deployed. This paper deals with the systematic investigation of impact of Silica Nanoparticles (Nano-SiO<sub>2</sub>) on the adsorption phenomenon of anionic surfactant Sodium dodecyl benzoic sulphonate (SDBS) in the reservoir core (RC) of Assam Shelf Basin. The adsorption of surfactant mostly relies on the clay type of RC, identified dominance clay was Kaolinite using scanning electron microscope (SEM) and X-ray diffraction (XRD) analysis. The experimental data obtained from adsorption experimental investigation were interpreted with adsorption isotherm models based on regression coefficient and isotherm showed addition of Nano-SiO2 shifted from Freundlich to Langmuir isotherm, whether the adsorption is multilayered to monolayered. We examined the stability of Nano -SiO2 in SDBS in acidic and basic medium was evaluated by measuring absorbance, zeta potential (ZP), particle size (PS) and wettability measurement (WA) by Contact angle (CA). The core flooding experiments were conducted and results found better recovery in case the slug 0.2 wt % SDBS+0.05 wt% Nano-SiO<sub>2</sub> in 3000 ppm NaCl about to 34.89% (PV 5.9 cc) of IOIP (PV 16.91 cc) as compared to the slug 0.2 wt% SDBS in 3000 ppm NaCl about to 24.84% (PV 4.2 cc) of IOIP. This work suggests the appropriate slug to be used for chemical flooding in the oil field of Assam Shelf Basin for effective CEOR.

**Keywords:** Anionic surfactant SDBS, Nano-SiO<sub>2</sub>, XRD, SEM, Adsorption, Isotherms, ZP, PS, CA, CEOR.

## 1. Introduction

As the petroleum reservoirs get matured the efficiency of production rate usually declines and ceases after some years [1]. So, to completely squeeze out the crude oil whichever is left over in the matured reservoirs some EOR techniques are to be deployed [2-3]. EOR techniques involve huge investment to increase the productivity of oil in depleted reservoirs. Surfactant flooding is the major employed CEOR method to produce hydrocarbons left over in the mature oil fields. Surfactants are more expensive than crude oil (CO), the development of a surfactant

flooding technique depends on how much surfactant can be economically sacrificed in recovering additional CO from a reservoir [4]. Adsorption of surfactant onto the rock surfaces of a reservoir limits the efficiency of the CEOR method deployed. As adsorption of surfactant initiates, the maximum utilization of surfactant for the reduction of interfacial tension (IFT) decreases [5]. A successful surfactant flooding process depends on the degree of retention of surfactants during flooding [6]. The quality amount of surfactant adsorbed depends on the rock properties like surface charges, surfactant characteristics, temperature, and salinity and pH value [7]. The reservoirs of Assam Shelf Basin are mostly sandstone reservoirs [8-10], so these reservoirs contain high amount of quartz (silica) and less amount of silicate and carbonate rock crystals. As silica is negatively (- ve) charged, the rock surfaces are also of (-ve) charge. So anionic surfactant is the most suitable surfactant to flood in the sandstone reservoirs [11] as it reduces the attraction of the surfactant towards rock surface and minimizes the chances of adsorption. To raise the efficiency of the surfactant, ph is altered by addition of different alkalis to the surfactant flooded [12-14] as the (-ve) charge on rock surfaces gets increased on addition of alkali ultimately adsorption can be minimized.

The addition of Nano-SiO<sub>2</sub> to surfactant flooding also modifies the surface charges of the rocks in the reservoir in such a way which further enhances the (-ve) charge originating from the clay-rich rocks preventing the attachment of the surfactants to the rock surface due to electrostatic repulsion [15]. The surfactant molecules are dispersed within the Nano-SiO<sub>2</sub> particles which synthesizes into an emulsion suitable for targeting reservoir rocks with spaced surfaces of low surface area of treated rock toward higher concentration of surfactants enabling mobility and accessibility at the oil-water interface [16]. The role of Nano-SiO2 is to control the surfactant tendency to aggregate and the formation of micelles on the rock surface. In the process of several surfactant molecules aggregating into a large micelle, nanoparticles (NP) may break some of the large micelles on the rock surface into smaller micelles. Hence, larger clusters may not absorb the rock easily. The result is less total adsorption and a higher concentrated surfactant concentration in the bulk phase [17]. Nano-SiO<sub>2</sub> interacts with surfactant molecules, forming complexes among the surfactant and NP that inhibit adsorption of surfactant molecules on the rock surface. This decreases the tendency of surfactants to come together to form micelles, thus enhancing the low trend of adsorption and efficient concentration of surfactants. Additionally, Nano-SiO2 also increases the hydrophilic character of rock surface; it causes water-wet the reservoir thereby improving the efficiency of the surfactant in the EOR process [18]. ZP measures the electrical charge on particles, indicating their tendency to repel or aggregate. A high ZP leads to better dispersion and stability in solutions. In LSW, fewer ions screen electrostatic repulsion, resulting in a higher absolute ZP [19]. Anionic surfactants interact with Nano-SiO<sub>2</sub> particles based on their ZP, which is typically (-ve) under low salinity conditions. This leads to repulsion between the particles, reducing surfactants adsorption onto the rock surface. This reduces oil-water IFT and mobilizes trapped oil. This reduced adsorption also maintains higher surfactant availability, allowing surfactants to spread throughout the reservoir and improve oil displacement [20, 21]. In this paper, the adsorption processes the equilibrium relationships between adsorbents and adsorbates are described by adsorption isotherms. Two different adsorption isotherms, Langmuir (1916) and Freundlich (1959) are used to describe the adsorption phenomenon of

the surfactant on the RC. From the results of adsorption data, the best fitting isotherms were determined and the adsorption phenomenon of a particular surfactant and further addition Nano-SiO<sub>2</sub> to the surfactant in a particular reservoir were determined. Circuitously the work is carried out to provide a complementary study of surface charge, PS, CA, core flooding and adsorption of anionic surfactants with/without addition of Nano-SiO<sub>2</sub> on the RCs of Assam Shelf Basin and proposed desired slug to be flooded to have an effective EOR.

## 2. Materials and methods

## 2.1 Materials and instruments

**Table 1.** Instruments used while conducting experimental work

SN	Instrument	Model/Source
1	UV - Spectrophotometer	SHIMADZU, UV-Probe 2.42
2	Centrifuge	ELECTRA LAB CENTRIFUGE
3	Hot air oven	I-therm AI-7782
4	Sieve shaking machine	S.D. HARDSON & Co.
5	Magnetic Stirrer	TARSONS
6	XRD	Ridaku, Optima IV
7	SEM	JEOL, JSM 6390LV
8	ZP & PS	Litesizer 500, Anton Paar
9	PH meter	Ampereus yellow digital ph meter
10	Ultra Sonicator Probe	Electrosonic Industries
	type	
11	Core flooding System	GON Engineering works
12	CA measurements	Dino Lite Digital microscope image
		with Hamilton microsyringe model
		1005 LTR SYR

**Table 2.** Materials used while conducting experimental work

SN	Materials	Source
1	SDBS	Merck Life Science Private Limited, Mumbai, India
2	Nano-SiO2	Sisco Research Laboratories Pvt. Ltd.
3	NaCl	LOBAL CHEMIE, Mumbai, India
4	RC	Oil fields of Oil India Limited, Assam Shelf Basin, India

## 2.2 Methodology

## 2.2.1 Preparation of clean sand grains (adsorbent) for adsorption study

To achieve 60-70 mesh size sand grains for the adsorption investigation, RC samples as shown in Table 2 SN 4 were sieved in a sieve shaking machine. The powder that was collected in the PAN was then taken for XRD and SEM analysis. By settling and decanting, the 60-70 mesh size sand grains were repeatedly cleaned with distilled water (DW). Following the removal of the suspended particles, the remaining wet sand grains were dried in a dehumidifier at 80°C

until they reached a consistent weight. The adsorption SDBS was measured using a UV Spectrophotometer using the adsorbents, which were sand grains with a mesh size of 60–70.

## 2.2.2 XRD and SEM sample preparations

A few grams were taken for the pipetting method for XRD study, and 2-5 grams were taken for SEM analysis from the powder collected in the PAN, as mentioned in 2.2.1. Using the pipetting method, 1000 ml of DW and PAN-collected fine sand powder were combined in a one-liter measuring cylinder. The mixture was thoroughly stirred for five to ten minutes using a magnetic stirrer, and it was left undisturbed for an hour. 5 ml of the solution, or the supernant, were gathered in a small beaker. Because clays are lighter than other minerals, the supernatant was taken from the middle of the solution level from the top. This procedure was carried out repeatedly until a considerable number of samples were gathered that were adequate for the XRD experiment. XRD of the prepared sample was recorded in a range of Bragg angle ( $10^{0} \le 2e \le 75^{0}$ ) using Ridaku XRD measuring instrument and analyzed [22].

## 2.2.3 Contact Angle measurements

The cylindrical core discs with dimensions 3.80 cm dia and 1 cm thickness were prepared in the core cutting machine followed by end facing and grinding machines to make uniform surfaces. The core discs were cleaned in Soxhlet apparatus and dried at hot air oven at 60°C until constant weight gained. Dried core discs saturated with the formation water for 24hrs and then saturated with CO at reservoir temperature 75°C for 7 days. The formulated slugs were dropped from a microsyringe on the core discs. Snapshots of CA were measured using Dino-Lite digital microscope with image analysis software.

## 2.2.4 Sample preparation of Zeta potentials and Particle size analysis

The formulated slugs selected based on previous results were taken to evaluate ZP distributions and PS analysis before and after core flooding in the instrument LiteSizer500.

## 2.2.5 Core flooding experiments

The cleaned RC, which measured 3.65 cm in diameter, 7.1 cm in length, 176.11 g in weight, and had a porosity of 25.7%, was put into a Hassler-style core holder within the coreflooding apparatus when the reservoir was at 750C. The primary brine flooding was carried out until the RC was saturated with brine once temperature equilibrium was reached early on. Second, crude oil floods the RC until irreducible water remains. The initial oil saturation (Soi) during CO flooding was the amount of brine flush out. Following that, a secondary brine flood was used to recover the Soi from the RC. The residual oil saturation (Sor) was then estimated by deducting the oil that had been flushed out of the Soi after the brine had broken through entirely. To recover that Sor, the formulated slugs 0.2% w/v SDBS and 0.2 wt% SDBS + 0.05 wt% Nano-SiO<sub>2</sub> were injected into the RC one at a time. The percentage of residual oil recovery from the initial oil in place (IOIP) was then measured by calculated the recovered residual oil from the RC.

## 2.2.6 Preparation of Adsorbate for adsorption study

0.2~w/v% is the critical micelle concentration (CMC) of SDBS in 5000 ppm brine stock solution to match the reservoir salinity 5000 ppm. Six experimental samples were made from the stock solution concentrations of  $10\text{--}60~\mu\text{g/ml}$ , either with or without Nano-SiO<sub>2</sub>. For 30 minutes, an ultrasonicator was used to create a homogeneous combination of Nano-SiO<sub>2</sub> in stock solution. After adding 1 gram of adsorbents to 10 milliliters of adsorbate and letting them come into contact for an hour in a rotospin, the samples were centrifuged for 20 minutes at 3000 rpm. The Spectrum technique was used to determine the wavelength of SDBS (Cazedey and Salgado, 2012). Using a photometric approach in the UV Spectrophotometer to find the absorbance difference before and after adsorption. The amount of adsorbate adsorbed onto the adsorbents was ascertained. The amount of adsorbate adsorbed on the adsorbent,  $\Gamma$  (mg/g),

was calculated by mass balance equation (2):  $\Gamma = \frac{(c_o - c_e)V}{m}$ 

Where,  $\Gamma$  = amount of adsorbate adsorbed on the adsorbent,  $\mu g/g$ 

 $C_0$  = Initial concentrations of adsorbate (before adsorption),  $\mu g/ml$ 

 $C_e$  = Equilibrium concentration (after adsorption) (µg/ml)

V = Solution volume (ml)

M = Mass of adsorbent/particles (gm)

## 2.2.7 Adsorption Isotherms

Langmuir isotherm model [23]

Linear from: 
$$\frac{1}{\tau} = \frac{1}{\tau_{\text{max}}} + \frac{1}{\tau_{\text{max}} K_L c_e}$$

Where,  $K_L$  = Langmuir isotherm constant, L/mg;  $\Gamma_{max}$  = Maximum monolayer coverage capacity, mg/g. Langmuir isotherm is applicable for monolayer adsorption because of the homogeneous surface of a finite number of identical sites.

Freundlich isotherm model [24]

Linear from: 
$$\log \tau_e = \log K_f + \frac{1}{n} \log c_e$$

Where,  $K_f$  = Freundlich adsorption constants, mg/g and n = sorption intensity, Freundlich isotherm has been derived by assuming an exponentially decaying sorption site energy distribution. The Freundlich isotherm assumes that surfactant adsorption occurs on a heterogeneous surface by multilayer sorption.

## 3. Results and Discussion

#### 3.1 XRD and SEM Analysis

RC sample from depth (2680.75 – 2680.90) m were taken XRD and SEM analysis. XRD patterns consist of sharp peaks at specific diffraction angles with intensities. The highest intensities at specific diffraction angles were compared with the reference book and identified the type of clays present in the RC of Assam Shelf Basin [25].

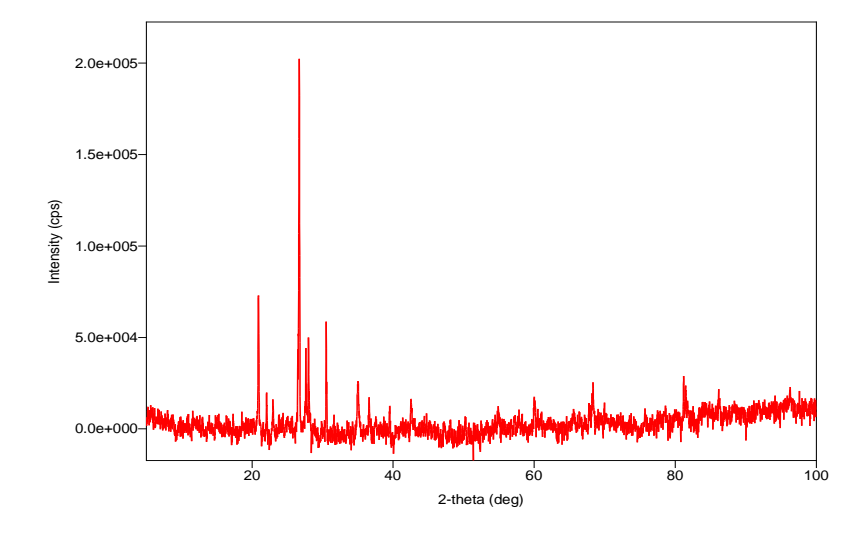


Fig.1 XRD result of RC

In Fig.1 peaks are single headed peak indicating no impurities in the sample which means the presence of a single phase. The characteristic picks were obtained at 21°, 27° and 28°. These 20 values were determined and was highest pick at 27° found Kaolinite as dominant clay mineral, other presence of clay minerals were montmorillonites and chlorite too. Several authors have attempted to address the effect of clay minerals presence on the adsorption of anionic surfactant with single adsorbent or clay fraction effect [26]. They reported that the kaolinite mineral has the highest adsorption, the impact of mineral surface area also affect adsorption, even with the (-ve) ions [27]. The effect of clay mineral's structure and surfactant nature on adsorption, very few researchers have studied the effect of montmorillonite and illite as single adsorbent on the anionic surfactant [28]. All the results show that electrostatic bond between the kaolinite mineral and the anionic surfactant is the dominant adsorption mechanism and very weak hydrogen bond with the other clay mineral [29]. SEM analysis revealed textures and structures that are invisible to the naked eye or conventional optical microscopes shown in Fig.2.

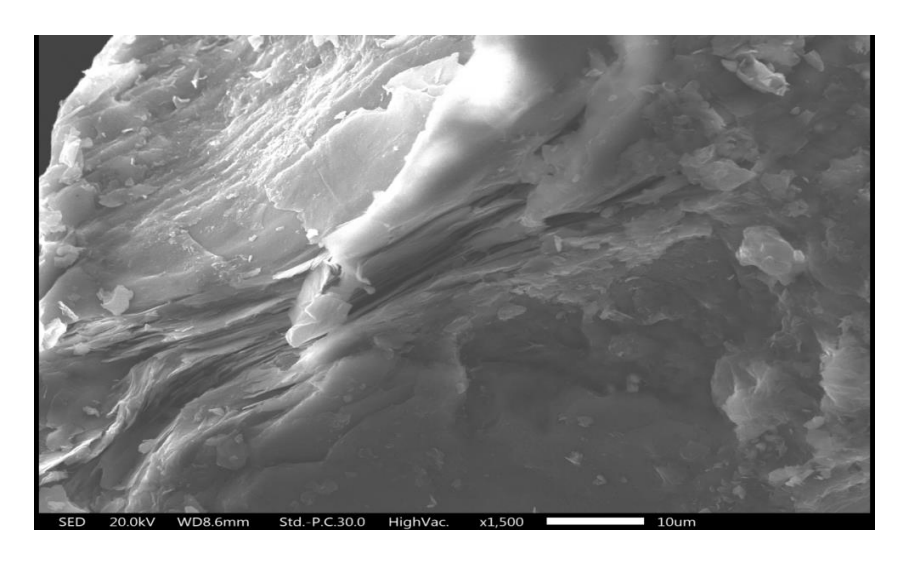


Fig.2 SEM image of RC

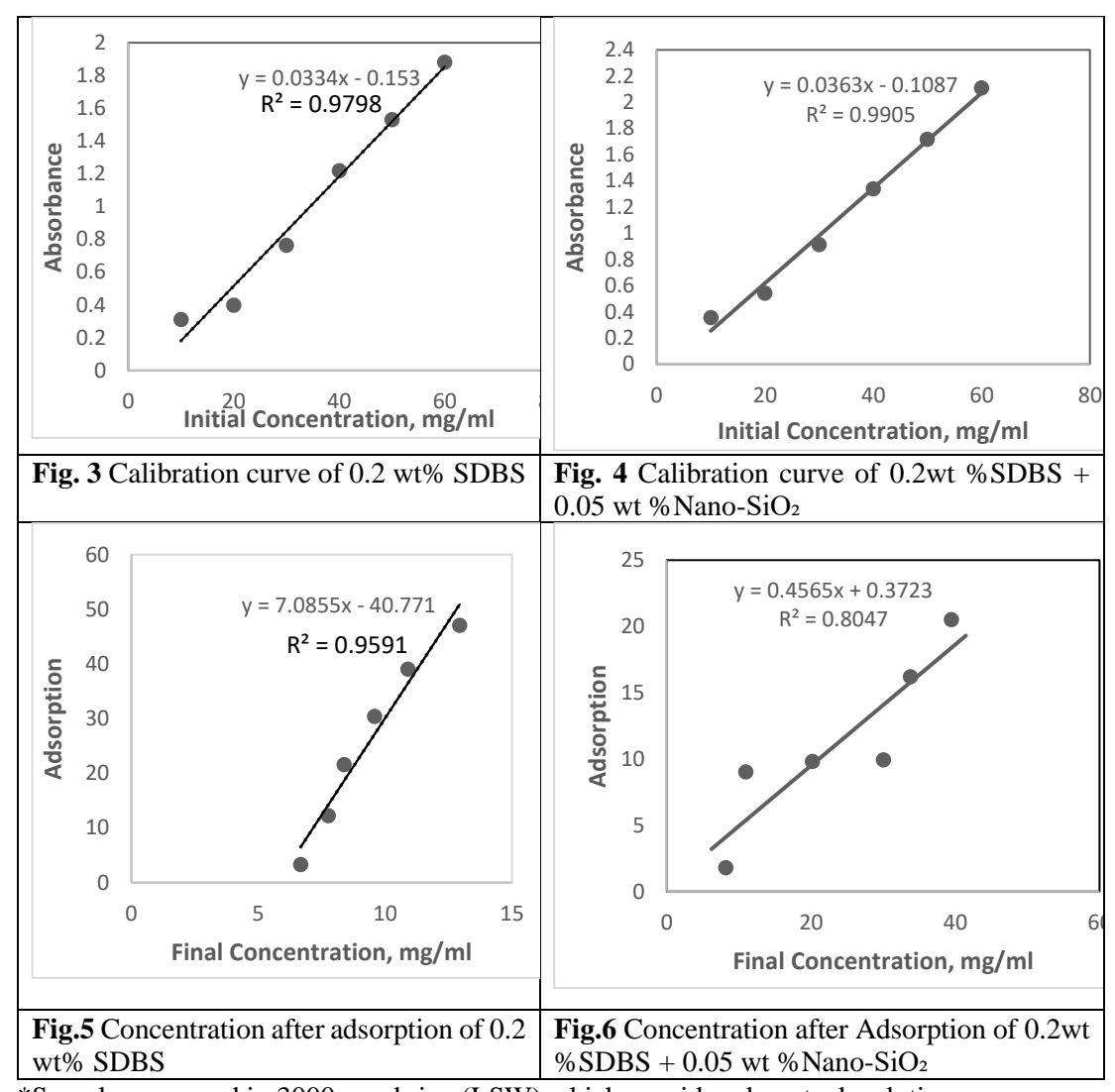
SEM image was analyzed [30] and revealed the presence of clay type Kaolinite. Kaolinite, a clay with a negative surface charge due to oxygen atoms, can exhibit positive charges under acidic conditions due to the loss of protons at higher pH levels and gain at lower pH levels [31]. This negatively affects the adsorption of cationic surfactants and can influence interactions with fluids and chemicals in acidic environments. The (-ve) charge during anionic surfactant flooding may lead to the repulsion of surfactants. Researchers [32, 33] have found that the adsorption effect in kaolinite-rich reservoirs can lower the effective concentration of surfactant for oil mobilization. To prevent loss, surfactant compositions could be modified with sacrificial agents and higher dosages. Anionic surfactants and Nano-SiO2 can alter wettability, promoting water-wet conditions. However, kaolinite can become mobile during fluid injection, leading to pore throat blockage or reduced permeability [34]. Optimizing the PS and concentration of Nano-SiO<sub>2</sub> in injected fluids can control their behaviour. Reservoir pH and ionic strength influence the surface charge of kaolinite and Nano-SiO<sub>2</sub>. Both aim to reduce IFT, improve wettability, and create favourable conditions for oil mobilization. Optimizing the concentration of both is critical for maximizing oil recovery in kaolinitedominant reservoirs. The ionic strength and salinity of fluids injected during EOR can also affect their performance [35]. Careful design of the surfactant and nanoparticle system is necessary to ensure sufficient active chemicals remain for altering interfacial properties.

#### 3.2 Adsorption Study

#### 3.2.1 Calibration Curve

The UV-VIS-Spectrophotometer is used to determine the absorbance of SDBS and SDBS + Nano-SiO<sub>2</sub> in 3000 ppm brine with or without an adsorbent. Plotting absorbance against concentration produced the calibration curves, which are displayed in figs (3, 4). The straight

line [y=mx+c] that represented the linear trend line needed to be calculated following the adsorption of surfactant on RC.



<sup>\*</sup>Samples prepared in 3000ppm brine (LSW) which considered as stock solution

From the calibration graphs Fig. (3 & 4) the equilibrium concentration i.e. the final concentration of the adsorbate was determined showed in Fig. (5 & 6) and values were shown in table 1 and presented decrease of adsorption values in percentage after addition Nano - SiO<sub>2</sub>.

**Table 1**. Final concentration and adsorption of the surfactant (SDBS)

0.2 wt% SDBS	0.2 wt% SDBS+ 0.05 wt% Nano-SiO2	
--------------	----------------------------------	--

Co, µg/ml	C <sub>e</sub> , µg/ml	Γ, μg/g	C <sub>e</sub> , µg/ml	Γ, μg/g	% of Decrease adsorption after addition Nano - SiO <sub>2</sub>
10	6.6766467	3.323353293	6.1625344	1.798898072	1.524
20	7.7544910	12.24550898	10.955922	9.044077135	3.201
30	8.3832335	21.61676647	20.184573	9.815426997	11.801
40	9.5808383	30.41916168	30.046831	9.953168044	20.466
50	10.898203	39.10179641	33.793388	16.20661157	22.895
60	12.934131	47.06586826	39.468319	20.53168044	26.534

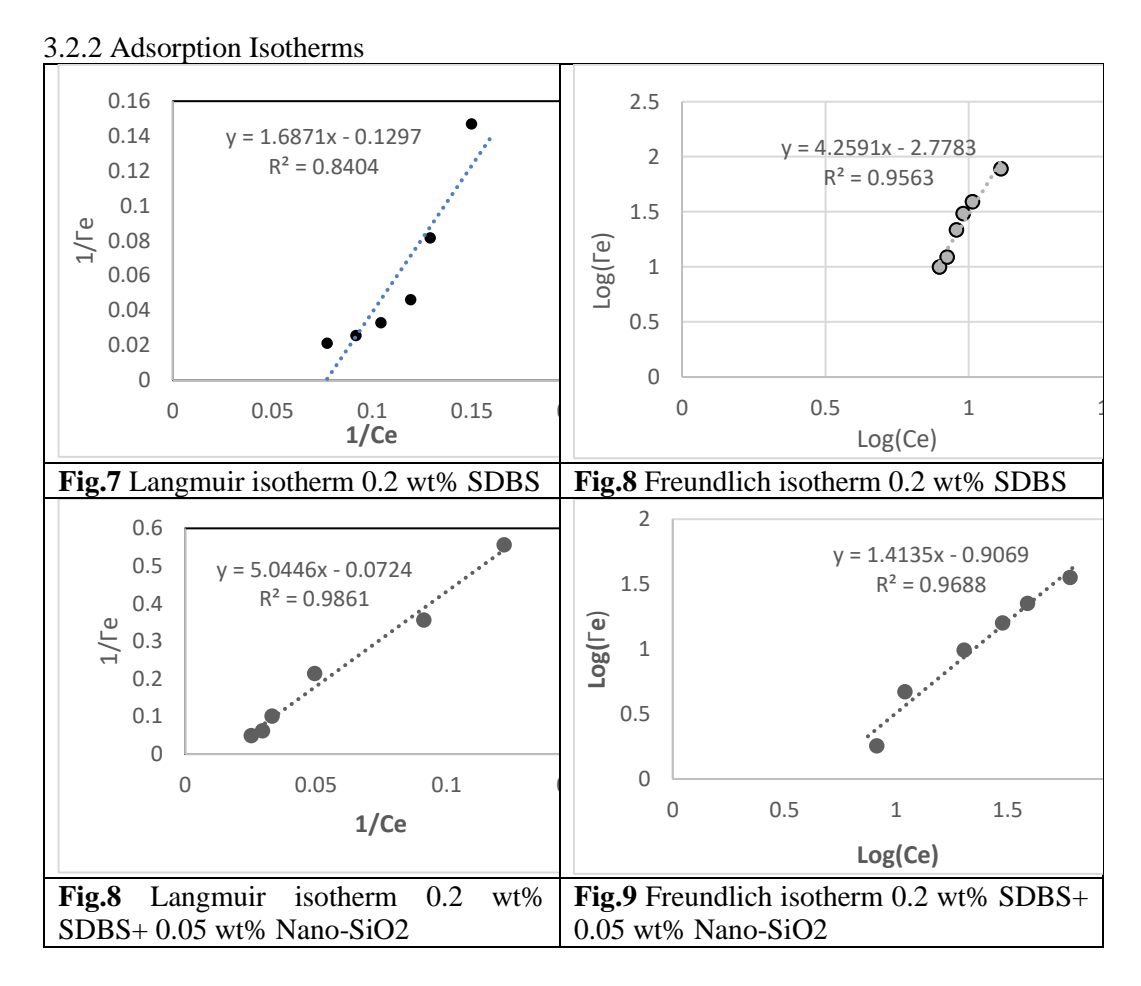


**Table 2.** Best fitted Isotherms

SN	Adsorbate	Langmuir, R <sup>2</sup>	Fruendlich, R <sup>2</sup>	<b>Best fitted Isotherm</b>
1	0.2 wt% SDBS	0.8404	0.9563	Freundlich
2	0.2 wt% SDBS+	0.9861	0.9688	
	0.05 wt% Nano-			Langmuir
	SiO2			

The study investigated the adsorption of 0.2 wt% SDBS and 0.2 wt% SDBS+ 0.05 wt% Nano-SiO2

on RC in the Assam Shelf Basin to evaluate surfactant flooding efficiency. The results showed that adsorption of surfactant onto the reservoir's clay led to a decrease in surfactant availability, reducing IFT and decreasing the efficiency of the EOR method. The major component of the clay is Kaolinite, as shown by XRD and SEM results. The adsorption phenomenon was described by Freundlich Isotherms, indicating a multilayered adsorption. However, when Nano-SiO<sub>2</sub> was added to SDBS solutions, the adsorption shifted towards monolayer adsorption is shown table2. In multilayered adsorption, surfactant adsorbed onto the mineral surface, while in monolayered adsorption, only a single layer of surfactant was adsorbed onto the mineral surface. When a site was occupied by solute, no further adsorption took place, resulting in a smaller amount of surfactant adsorption. The Freundlich isotherm is a widely used method for adsorption of surfactants onto solid surfaces. Without Nano-SiO2, the adsorption behaviour was heterogeneous multilayer adsorption with no sharp saturation point [36]. However, the addition of Nano-SiO<sub>2</sub> significantly changed the adsorption behaviour due to its large surface area, uniformly distributed active sites, and interaction with Nano-SiO<sub>2</sub>. This results in a monolayer adsorption mechanism, better explained by the Langmuir model. This shift in adsorption behaviour is crucial for optimizing surfactant adsorption during EOR operations, improving efficiency in reducing IFT and mobilizing trapped oil. The adsorption of surfactants in monolayered adsorption is significantly reduced when Nano - SiO2 is added to the surfactant solution is shown in table 1. The Freundlich isotherm is used for adsorption, but without Nano - SiO<sub>2</sub>, the adsorption behaviour is heterogeneous with no sharp saturation point. However, the addition of Nano - SiO<sub>2</sub> significantly changes the adsorption behaviour due to its large surface area, uniformly distributed active sites, and interaction with Nano -SiO<sub>2</sub>. This results in a monolayer adsorption mechanism, better explained by the Langmuir model. This shift in adsorption behaviour is crucial for optimizing surfactant adsorption during EOR operations, improving efficiency in reducing IFT and mobilizing trapped oil.

#### 3.3 ZP and PS

ZP measures the electrical charge on particles, indicating their tendency to repel or aggregate. A high ZP leads to better dispersion and stability in solutions by reducing IFT and capillary forces. The Fig (10, 11, 12 & 13) showed the variation of ZP of SDBS, SDBS + Nano- SiO<sub>2</sub>, SDBS + Nano- SiO<sub>2</sub>+RC and SDBS + Nano- SiO<sub>2</sub> + RC+ CO. The results can be observed that addition of Nano- SiO<sub>2</sub> with RC and RC + CO significantly titling (- ve) zeta values from -19.2 mv to -42.5 mv and -62.1 mv which impacts SDBS surfactant flooding by enhancing particle stability, reducing surfactant adsorption, improving wettability, and hence it will be preventing pore throat blockage [37, 38]. A negative surface charge is frequently present in the reservoir rock, particularly if it contains clays like kaolinite. In LSW, Nano- SiO<sub>2</sub> particles

with a high ZP repel one another and the rock surface, decreasing the likelihood of adsorption. This repulsion keeps SiO<sub>2</sub> from depositing on rock surfaces, preserving the NPs mobility and allowing them to efficiently change their WA from oil-wet to water-wet, improving oil displacement [39]. A negative charge is also present in anionic surfactants, so combination of Nano-SiO<sub>2</sub> and SDBS cause high (-ve) ZP aids to inhibit less adsorption onto the rock surfaces and retaining more surfactant in the injected fluid. Table 3 showed change of ZP and PS variation with the of PH.

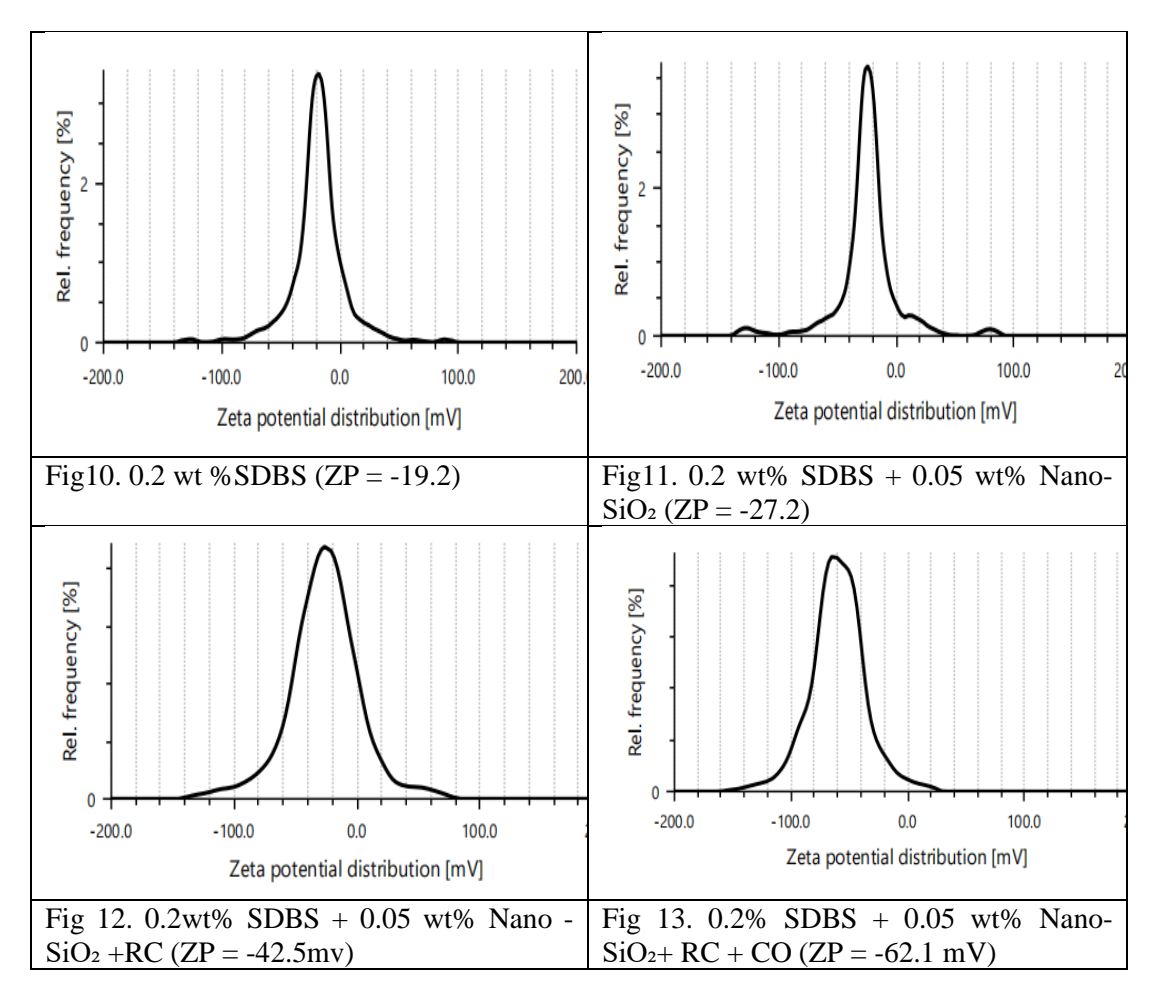


Table 3. ZP and PS variation with PH

S N		РН	ZP (mv)	PS (nm)
1	0.05 wt% Nano - SiO <sub>2</sub>	7.5	-19.2	73
2	$0.05$ wt% Nano - $SiO_2 + 0.2$ wt % SDBS	2.5	11.3	39

3	0.05 wt% Nano - SiO <sub>2</sub> + 0.2wt % SDBS	8.67	-27.2	102
4	0.05 wt% Nano - SiO <sub>2</sub> + 0.2wt % SDBS	11.89	-	Agglomerate

The study explores the stability of Nano-SiO2 in acidic and basic pH conditions, revealing that adjusting the pH significantly increases NP stability, as evidenced by a decrease in PS in table3. In LSW, increased ZP on Nano-SiO<sub>2</sub> surfaces aids in uniform particle spread and improves oil displacement efficiency. The interaction between Nano-SiO2 and (-ve)ly charged rock surfaces, like kaolinite-rich formations, is influenced by the ZP, creating electrostatic repulsion [40]. LSW flooding leads to a decrease in ionic strength, resulting in an increase in the electric double layer around Nano-SiO<sub>2</sub> particles and RC. Further addition of Nano-SiO<sub>2</sub>, this layer associated with higher absolute ZP -27.2 mv, reduces the adsorption of SDBS onto rock surfaces, allowing more surfactant to remain in the solution and improving oil mobilization. High ZP ensures Nano- SiO<sub>2</sub> particles remain well-dispersed and interact more efficiently with trapped oil and rock surfaces, reducing oil-water IFT and promoting oil flow towards production wells [41]. For EOR, Nano-SiO2 assisted anionic surfactant flooding relies heavily on ZP and PS. A high (-ve) ZP promotes particle stability, inhibits aggregation, and enhances surfactant and Nano-SiO<sub>2</sub>, mobility. To prevent pore blockage, small particle size improves pore accessibility, lowers IFT, and encourages greater oil displacement. By encouraging efficient oil mobilization, enhancing sweep efficiency, and averting problems with particle aggregation or pore plugging, these elements guarantee optimal performance in EOR and raise oil recovery efficiency [42].

3.4 Contact Angle (CA) measurements

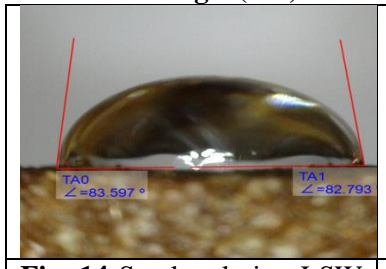


**Fig. 14** Stock solution LSW (3000 ppm NaCl) Avg. CA= 83.195°

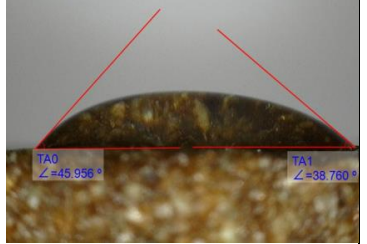


**Fig.15** 0.2 wt% SDBS Avg. CA= 42.358°

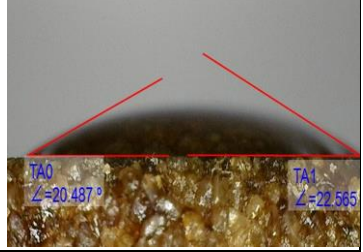


**Fig.16** 0.2 wt% SDBS + 0.05 wt% Nano-SiO<sub>2</sub>; Avg. CA= 21.526°

The CA measurement in the context of Nano- SiO<sub>2</sub> aided surfactant flooding in LSW plays a key role in understanding the WA of the RC. The CA of LSW reduces from 83.195° to 42.358° and 21.526° addition of 0.2 wt% SDBS and 0.2 wt% SDBS + 0.05 wt% Nano- SiO<sub>2</sub> shown in fig (14, 15 &16). The CA determines whether a surface is wettable and whether the rock is water-, oil-, or mixed-wet. The objective of EOR is frequently to increase oil recovery by changing the WA from an oil-wet or mixed-wet state to a more water wet [43]. Oil is more likely to stick to the rock surface and prevent water from dislodging it when the CA is high

(>90°). Water can more readily spread across the rock surface in a water-wet condition when the CA is low (less than 90°). By decreasing the CA, the goal of nano- SiO<sub>2</sub> assisted surfactant flooding with LSW is to change the wettability of the rock toward a more water-wet condition [44, 45]. As a result, the injected water can drive oil through the reservoir more efficiently, improving oil displacement. The capillary forces (CF) in the reservoir are lessened when the CA is smaller. Less CF allow trapped oil to be more readily displaced by the injected LSW and the surfactant-nano-silica mixture. As the CA decreases, the tendency of water to spread across the rock surface increases, improving the mobility of oil within the pore spaces [46]. Because more oil may flow towards production wells because of this greater displacement, oil recovery is improved.

## 3.5 Core flooding

Core flood experiments aim to estimate the total amount of co recovered from secondary and tertiary recovery. The experiments were conducted using Johnson, Bossler, and Naumann (JBN) techniques and reservoir core from depth of 2533-2533.15 m of having porosity 25.7%. A synthetic brine solution of 3000 ppm NaCl was used for primary and secondary recovery, and CO from the same formation was used for oil flooding to meet the compositions that exists in the reservoir. Table 4 showed the recovery of each 0.2 wt% SDBS in 3000 NaCl slug out of initial oil in place (IOIP). The mixed slug 0.2 wt % SDBS+0.05 wt% Nano-SiO<sub>2</sub> in 3000 ppm was recovered more about to 34.89% (PV 5.9 cc) of IOIP (PV 16.91 cc) as compared to the slug 0.2 wt% SDBS in 3000 NaCl about to 24.84% (PV 4.2 cc) of IOIP. The mixed slug was recovered more than the slug 0.2 wt% SDBS in 3000 NaCl.

Table 4. Total flood volumes for Secondary and Tertiary recovery

Reservoir core (PV 19.57 cc)		
Initial oil saturation, Soi (PV 16.91 cc) + Irreducible water saturation, Swc (PV 2.66 cc)		
Primary +Secondary recovery from initial Residual oil left		
oil saturation53% of IOIP (PV 9.01cc)	46.72 of IOIP, (PV 7	7.9 cc)
Formulated Slug	Recovered oil, %	Unrecovered, %
	IOIP	IOIP
0.2 wt% SDBS + 3000 ppm NaCl 0.2 wt% SDBS + 0.05 wt % NP +3000 ppm NaCl	24.84 % IOIP (PV 4.2 cc) 34.89 % IOIP (PV 5.9 cc)	21.88 % IOIP (PV 3.7 cc) 11.83 % IOIP (PV 2 cc)

The cumulative amount of residual oil recovered out of residual oil in place (ROIP) was plotted against the pore volume introduced into the core flooding system in Figure 17. In contrast to the slug 0.2 Wt % SDBS + 3000 ppm NaCl, which recovered 53.16 % ROIP percent after the injection of 100% formulated slug, the results indicated that the slug 0.2 wt% SDBS + 0.05 wt% Nano-SiO<sub>2</sub> + 3000 ppm NaCl provided a greater recovery, 74.8% ROIP.

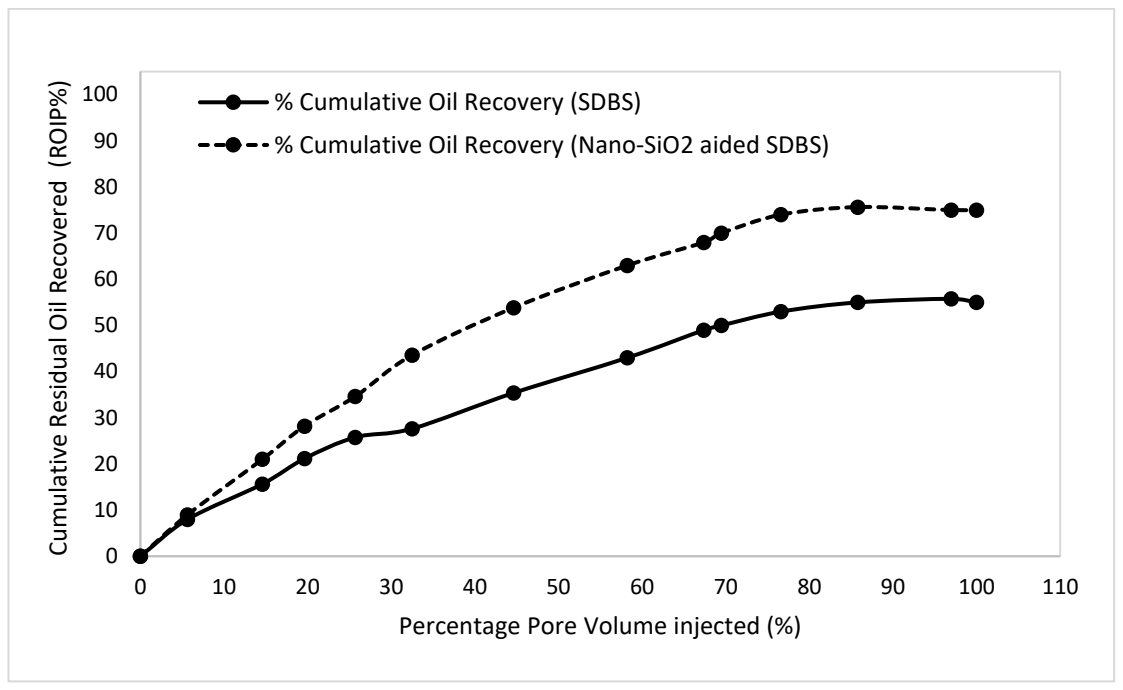


Fig. 17 Cumulative Residual Oil Saturation recovered vs formulated slugs injected

#### 4. CONCLUSION

The findings of this study are as follows:

- The RC showed mostly Kaolinite dominant clay present from XRD and SEM analysis which indicates the reservoir is anionic in nature.
- The rate of adsorption depends on availability of surfactant in the system; it was found that the adsorption of surfactant increased with increasing surfactant concentration.
- The SDBS showed the best fitted isotherm with Freundlich Adsorption Isotherm which indicates the multilayered adsorption of surfactant on the RC. Further, addition of 0.5 wt% Nano-SiO<sub>2</sub> to 0.2 wt% SDBS solution, the adsorption shifted towards monolayer adsorption isotherm. The effect of addition of Nano-SiO<sub>2</sub> to 0.2 wt% SDBS solution reduces the significant adsorption of SDBS surfactant on the RC.
- 0.05 wt% Nano SiO<sub>2</sub> + 0.2wt % SDBS with ph 8.67 showed (-) ve ZP compared with 0.05 wt% Nano SiO<sub>2</sub> + 0.2wt % SDBS of ph 2.5 and 0.05 wt% Nano SiO<sub>2</sub> of ph 7.5. A high ZP promotes particle stability, inhibits aggregation and less adsorption of slug in RC.
- The CA measurement of LSW reduced from 83.195° to 42.358° and 21.526° when added 0.2 wt % SDBS and 0.2 wt #% SDBS + 0.05 wt% Nano SiO<sub>2</sub>. The mixed slug showed WA towards more water wet.

- The mixed slug 0.2 wt % SDBS+0.05 wt% Nano-SiO<sub>2</sub> in 3000 ppm was recovered more about to 34.89% (PV 5.9 cc) of IOIP (PV 16.91 cc) as compared to the slug 0.2 wt% SDBS in 3000 NaCl about to 24.84% (PV 4.2 cc) of IOIP. The mixed slug was recovered more than the slug 0.2 wt% SDBS.
- The best slug found to be 0.2 wt % SDBS+0.05 wt% Nano-SiO<sub>2</sub> based on experimental analysis adsorption study, ZP, PS, CA and core flooding.

## Acknowledgment

The Authors would like to express their sincere gratitude to the Department of Chemistry, Department of Petroleum Technology and Department of Petroleum Engineering of Dibrugarh University for providing the excess of institutional facilities and resources to carry out the work without which this work would not have been possible.

## **Nomenclature**

CEOR Chemical Enhanced Oil Recovery SEM Scanning Electron microscope

XRD X-ray diffraction Nano-SiO<sub>2</sub> Silica Nanoparticles

SDBS Sodium dodecyl benzoic sulphonate

NaCl Sodium Cloride RC Reservoir Core CO Crude Oil

WA Wettability Alternation

ZP Zeta Potential
PS Particle Size
IFT Interfacial Tension
DW Distilled Water
LSW Low Salinity Water
NP Nanoparticles

Negative (-) ve

IOIP Initial Oil in Place ROIP Residual Oil in Place

CA Contact angle PV Pore volume

Soi Initial Oil Saturation Sor Residual Oil Saturation EOR Enhanced Oil Recovery

CF Capillary Force

#### References

- 1. Hirasaki G.J., Miller C. A., Puerto M. (2008), Recent advances in surfactant EOR. in SPE Annual Technical Conference and Exhibition. Society of Petroleum Engineers, USA, pp 35
- 2. Shahs D.O., (1981), Surface phenomena in enhanced oil recovery. In: Dinesh O Shah Springer US, ISBN: 978-1-4757-0337-5.
- 3. Hanna H., Somasundaran P. (1977), Physico-chemical aspects of adsorption at solid/liquid interfaces. II. Mahogany sulfonate/berea sandstone, kaolinite. Academic Press, New York, USA
- 4. Amyx J.W., Bass D.M., Whiting R.L., (1960), Petroleum reservoir engineering: physical properties. McGraw-Hill College, p. 610.
- 5. Dorothy C., (1970), Clay minerals: A guide to their X-ray identification, The Geological society of America, Special Paper 126.
- 6. Langmuir. I., 1916, The constitution and fundamental properties of solids and liquids. J.Am.Chem.Soc., 38, 2221.
- 7. Investigation of Adsorption of Surfactants onto Illite and Relations to Enhanced Oil Recovery Methods, Ingrid Karlsen Hov, Department of Chemical Engineering, Norwegian University of Science and Technology.
- 8. Mazen Ahmed Muherei, Radzuan Junin, Equilibrium Adsorption Isotherms of Anionic, Nonionic Surfactants and Their Mixtures to Shale and Sandstone, vol (3), no.(2), Modern Applied Sciences Feb 2009.
- 9. Ziegler V.M, Handy LL (1981) Effect of temperature on surfactant adsorption in porous media. Society of Petroleum Engineers Journal 21(02): 218-228.
- 10. McGuire, P. L.; Chatham, J. R.; Paskvan, F. K.; Sommer, D. M.; Carini, F. H. Low Salinity Oil Recovery: An Exciting New EOR Opportunity for Alaska's North Slope. SPE Western Regional Meeting: Irvine, California, U.S.A., 30 March—1 April, 2005.
- 11. Behera, U. S.; Sangwai, J. S. Nanofluids of Silica Nanoparticles in Low Salinity Water with Surfactant and Polymer (SMART LowSal) for Enhanced Oil Recovery. J. Mol. Liq. 2021, 342, 117388.
- 12. Rosen, M. J.; Wang, H.; Shen, P.; Zhu, Y. Ultralow Interfacial Tension for Enhanced Oil Recovery at Very Low Surfactant Concentrations. Langmuir 2005, 21, 3749–3756.
- 13. Friedmann, F. Surfactant and Polymer Losses During Flow Through Porous Media. SPE Reservoir Eng. 1986, 1, 261–271.
- 14. Alagic, E.; Spildo, K.; Skauge, A.; Solbakken, J. Effect of Crude Oil Ageing on Low Salinity and Low Salinity Surfactant Flooding. J. Pet. Sci. Eng. 2011, 78, 220–227.
- 15. Lugo, D. M.; Oberdisse, J.; Lapp, A.; Findenegg, G. H. Effect of Nanoparticle Size on the Morphology of Adsorbed Surfactant Layers. J. Phys. Chem. B 2010, 114, 4183–4191.
- 16. Ahmadi, M. A.; Sheng, J. Performance Improvement of Ionic Surfactant Flooding in Carbonate Rock Samples by Use of Nanoparticles. Pet. Sci. 2016, 13, 725–736.
- 17. Kumar, G.; Kakati, A.; Mani, E.; Sangwai, J. S. Stability of Nanoparticle Stabilized Oilin-Water Pickering Emulsion under High Pressure and High Temperature Conditions: Comparison with Surfactant Stabilized Oil-in-Water Emulsion. J. Dispersion Sci. Technol. 2021, 42, 1204–1217.

- 18. Yousefvand, H. A.; Jafari, A. Stability and Flooding Analysis of Nanosilica/NaCl /HPAM/SDS Solution for Enhanced Heavy Oil Recovery. J. Pet. Sci. Eng. 2018, 162, 283–291.
- 19. Kim, I.; Taghavy, A.; DiCarlo, D.; Huh, C. Aggregation of Silica Nanoparticles and Its Impact on Particle Mobility under High-Salinity Conditions. J. Pet. Sci. Eng. 2015, 133, 376–383.
- 20. Choudhary, R.; Khurana, D.; Kumar, A.; Subudhi, S. Stability Analysis of Al2O3 /Water Nanofluids. J. Exp. Nanosci. 2017, 12, 140–151.
- 21. Al-Anssari, S.; Barifcani, A.; Wang, S.; Maxim, L.; Iglauer, S. Wettability Alteration of Oil-Wet Carbonate by Silica Nanofluid. J. Colloid Interface Sci. 2016, 461, 435–442.
- 22. Maurice Tucker, Techniques in Sedimentology 1998 https://www.researchgate.net/publication/285864992\_Techniques\_in\_Sedimentology
- 23. Langmuir, I. The constitution and fundamental properties of solids and liquids. J.Am.Chem.Soc., 1916, 38, 2221.
- 24. Mazen Ahmed Muherei, Radzuan Junin, Equilibrium Adsorption Isotherms of Anionic, Nonionic Surfactants and Their Mixtures to Shale and Sandstone, vol (3), no. (2), Modern Applied Sciences Feb 2009.
- 25. Dorothy C. Clay minerals: A guide to their X-ray identification, The Geological society of America, 1970, Special Paper 126.
- 26. Amyx J.W., Bass D.M., Whiting R.L. Petroleum reservoir engineering: physical properties. McGraw-Hill College, 1960, p. 610.
- 27. Ziegler V.M, Handy LL (1981) Effect of temperature on surfactant adsorption in porous media. Society of Petroleum Engineers Journal 21(02): 218-228.
- 28. Maghzi, A.; Mohammadi, S.; Ghazanfari, M. H.; Kharrat, R.; Masihi, M. Monitoring Wettability Alteration by Silica Nanoparticles during Water Flooding to Heavy Oils in Five-Spot Systems: A Pore- Level Investigation. Exp. Therm. Fluid Sci. 2012, 40, 168–176.
- 29. Hou, B.; Jia, R.; Fu, M.; Li, L.; Xu, T.; Jiang, C. Mechanism of Synergistically Changing Wettability of an Oil-Wet Sandstone Surface by a Novel Nanoactive Fluid. Energy Fuels 2020, 34, 6871–6878.
- 30. Rezvani, H.; Riazi, M.; Tabaei, M.; Kazemzadeh, Y.; Sharifi, M. Experimental Investigation of Interfacial Properties in the EOR Mechanisms by the Novel Synthesized Fe3O4@Chitosan Nanocomposites. Colloids Surf., A 2018, 544, 15–27.
- 31. Kazemzadeh, Y.; Sharifi, M.; Riazi, M.; Rezvani, H.; Tabaei, M. Potential Effects of Metal Oxide/SiO2 Nanocomposites in EOR Processes at Different Pressures. Colloids Surf., A 2018, 559, 372–384.
- 32. Austad, T.; Matre, B.; Milter, J.; Savareid, A.; Oyno, L. Chemical Flooding of Oil Reservoirs 8. Spontaneous Oil Expulsion from Oil- and Water-Wet Low Permeable Chalk Material by Imbibition of Aqueous Surfactant Solutions. Colloids Surf., A 1998, 137, 117–129.
- 33. Cheraghian, G.; Kiani, S.; Nassar, N. N.; Alexander, S.; Barron, A. R. Silica Nanoparticle Enhancement in the Efficiency of Surfactant Flooding of Heavy Oil in a Glass Micromodel. Ind. Eng. Chem. Res. 2017, 56, 8528–8534.

- 34. Binks, B. P.; Rodrigues, J. A.; Frith, W. J. Synergistic Interaction in Emulsions Stabilized by a Mixture of Silica Nanoparticles and Cationic Surfactant. Langmuir 2007, 23, 3626–3636.
- 35. Rezaei, A.; Riazi, M.; Escrochi, M.; Elhaei, R. Integrating Surfactant, Alkali and Nano-Fluid Flooding for Enhanced Oil Recovery: A Mechanistic Experimental Study of Novel Chemical Combinations. J. Mol. Liq. 2020, 308, 113106.
- 36. Yekeen, N.; Padmanabhan, E.; Syed, A. H.; Sevoo, T.; Kanesen, K. Synergistic Influence of Nanoparticles and Surfactants on Interfacial Tension Reduction, Wettability Alteration and Stabilization of Oil-in-Water Emulsion. J. Pet. Sci. Eng. 2020, 186, 106779.
- 37. Liu, S., Hu, Y., Xia, J., Fang, S., Duan, M., 2019. In situ measurement of depletion caused by SDBS micelles on the surface of silica particles using optical tweezers. Langmuir 35 (42), 13536–13542.
- 38. Liu, Z., Bode, V., Hadayati, P., Onay, H., Sudh olter, E.J., 2020. Understanding the stability mechanism of silica nanoparticles: the effect of cations and EOR chemicals. Fuel 280, 118650.
- 39. Maghzi, A., Mohammadi, S., Ghazanfari, M.H., Kharrat, R., Masihi, M., 2012. Monitoring wettability alteration by silica nanoparticles during water flooding to heavy oils in five-spot systems: a pore-level investigation. Exp. Therm. Fluid Sci. 40, 168–176.
- 40. Mohajeri, M., Rasaei, M.R., Hekmatzadeh, M., 2019. Experimental study on using SiO2 nanoparticles along with surfactant in an EOR process in micromodel. Petrol. Res. 4 (1), 59–70.
- 41. Mukherjee, S., Paria, S., 2013. Preparation and stability of nanofluids-a review. IOSR J. Mech. Civ. Eng. 9 (2), 63–69.
- 42. Nasralla, R.A., Bataweel, M.A., Nasr-El-Din, H.A., 2013. Investigation of wettability alteration and oil-recovery improvement by low-salinity water in sandstone rock. J. Can. Petrol. Technol. 52 (2), 144–154.
- 43. Nwidee, L.N., et al., 2017a. Nanoparticles influence on wetting behaviour of fractured limestone formation. J. Petrol. Sci. Eng. 149, 782–788.
- 44. Nwidee, L.N., Lebedev, M., Barifcani, A., Sarmadivaleh, M., Iglauer, S., 2017b. Wettability alteration of oil-wet limestone using surfactant-nanoparticle formulation. J. Colloid Interface Sci. 504, 334–345.
- 45. Philippe, A., Schaumann, G.E., 2014. Interactions of dissolved organic matter with natural and engineered inorganic colloids: a review. Environ. Sci. Technol. 48 (16), 8946–8962.
- 46. Pooryousefy, E., Xie, Q., Chen, Y., Sari, A., Saeedi, A., 2018. Drivers of low salinity effect in sandstone reservoirs. J. Mol. Liq. 250, 396–403.
- 47. Radelczuk, H., Holysz, L., Chibowski, E., 2002. Comparison of the Lifshitz-van der Waals/acid-base and contact angle hysteresis approaches for determination of solid surface free energy. J. Adhes. Sci. Technol. 16 (12), 1547–1568.
- 48. Rausch, R., Beaver, K., 1964. Case history of successfully water flooding a fractured sandstone. J. Petrol. Technol. 16 (11), 1233–1237.
- 49. Rosen, M.J., Kunjappu, J.T., 2012. Surfactants and Interfacial Phenomena.
- 50. John Wiley & Sons. Sadeghi, R., Etemad, S.G., Keshavarzi, E., Haghshenasfard, M., 2015. Investigation of alumina nanofluid stability by UV-vis spectrum. Microfluid. Nanofluidics 18 (5), 1023–1030.

Application Of Silica Nanoparticles And Joyshree Barman et al. 1208